Lipids in Health and Disease

RESEARCH

Open Access

Ergothioneine ameliorates metabolic dysfunction-Associated Steatotic Liver Disease (MASLD) by enhancing autophagy, inhibiting oxidative damage and inflammation

Xiaoyu Lv[1], Chenyu Nie[1], Yihan Shi[1], Qincheng Qiao[1], Jing Gao[1], Ying Zou[1], Jingwen Yang[1], Li Chen[1,2,3,4] and Xinguo Hou[1,2,3,4*]

Abstract

Background Metabolic dysfunction-associated steatosis liver disease (MASLD) is one of the most common metabolic liver diseases around the world, whose prevalence continues to increase. Currently, there are few medications to treat MASLD. Ergothioneine is a natural compound derived from mushrooms whose sulfhydryl groups confer unique antioxidant, anti-inflammatory and detoxifying effects. Currently, research on the therapeutic effects of ergothioneine in MASLD is unknown. Therefore, this study explored the effect and mechanism of EGT in MASLD.

Methods The ameliorative effects and mechanisms of ergothioneine on MASLD were evaluated using HFD mice and PA-treated AML12 cells. Mouse body weight, body fat, IPGTT, IPITT, immunohistochemistry, serum biochemical indices, and staining of liver sections were assayed to verify the protective role of ergothioneine in MASLD. RNA-seq was applied to explore the mechanism of action of ergothioneine. The role of ergothioneine in AML12 was confirmed by western blotting, qPCR, ELISA, Oil Red O staining, flow cytometry, and ROS assays. Subsequently, the 3-methyladenine (3-MA, an autophagy inhibitor) was subsequently used to confirm that ergothioneine alleviated MASLD by promoting autophagy.

Results Ergothioneine reduced body weight, body fat and blood lipids, and improved insulin resistance and lipid and glycogen deposition in MASLD mice. Furthermore, ergothioneine was found to increase autophagy levels and attenuate oxidative damage, inflammation, and apoptosis. In contrast, intervention with 3-MA abrogated these effects, suggesting that ergothioneine ameliorated effects by promoting autophagy.

Conclusion Ergothioneine may be a drug with great therapeutic potential for MASLD. Furthermore, this protective effect was mediated through the activation of autophagy.

Keywords Ergothioneine, MASLD, Autophagy, Lipid metabolism, Apoptosis, Oxidative stress

*Correspondence:
Xinguo Hou
houxinguo@sdu.edu.cn
[1]Department of Endocrinology, Cheeloo College of Medicine, Qilu Hospital of Shandong University, Shandong University, 107 Wenhuaxi Road, Li Xia district, Jinan, Shandong 250012, China
[2]Institute of Endocrine and Metabolic Diseases of Shandong University, Jinan, Shandong 250012, China
[3]Key Laboratory of Endocrine and Metabolic Diseases, Shandong Province Medicine & Health, Jinan, Shandong 250012, China
[4]Jinan Clinical Research Center for Endocrine and Metabolic Disease, Jinan, Shandong 250012, China

Introduction

As recently as 2023, the multisociety Delphi consensus statement replaced the nomenclature of metabolic dysfunction-associated fatty liver disease (MAFLD) with MASLD [1]. MASLD is one of the most common metabolic syndromes worldwide, whose prevalence continues to increase [2]. MASLD may develop to metabolic dysfunction-associated steatohepatitis, cirrhosis, and hepatocellular carcinoma [3–5]. Additionally, MASLD is associated with various metabolic diseases, including cardiovascular complications, obesity, and type 2 diabetes mellitus [6]. In recent years, MASLD has affected approximately 24% the population and become a widespread metabolic disease in the earth [7, 8]. However, few specific medications are currently available to treat MASLD [9, 10].

The pathologic mechanism of MASLD is still unclear, but various factors affecting hepatic lipid metabolism may promote the development of fatty liver. Current studies on MASLD have shown that insulin resistance (IR) and hepatic fat accumulation are among the most important pathogenic mechanisms [11, 12]. In addition, oxidative stress and inflammatory responses caused by lipotoxicity can also lead to liver damage and worsen the progression of MASLD [13].

Autophagy is a conserved process essential for maintaining the stability of the intracellular environment. In this process, cells phagocytose their cytoplasmic proteins or organelles and encapsulate them into vesicles, then, vesicles and lysosomes are fused to autolysosomes that degrade their encapsulated contents, thereby accomplishing cellular self-renewal and repair [14]. This process generally consists of induction, initial nucleation, autophagosome formation, binding to lysosomes, and finally digestion. Autophagy-associated (ATG) proteins are crucial for this process [15]. In recent years, autophagy shows a vital effect in regulating lipid metabolism of liver [16, 17]. Activation of autophagy can regulate the expression of lipid metabolism genes to decline lipid content, whereas inhibition of autophagy can contribute to lipids overaccumulation [18, 19]. In addition, restoration of autophagic flux can attenuate MASLD [19–22]. Therefore, substances that promote autophagy activation have great potential for the treatment of MASLD.

Ergothioneine (EGT) is a natural histidine thiourea derivative originated primarily from bacteria and fungus [23–25]. The sulfhydryl groups in EGT have a number of beneficial effects, including antioxidant, anti-inflammatory, and antidote action that protect against damage to organisms [26]. The unique properties of EGT make it a very potent antioxidant and cytoprotective agent [27, 28]. At the present, some studies have verified that EGT has preventive or therapeutic potential for a range of oxidative stress-related diseases [27, 29], and the liver has been shown to be an important organ of EGT accumulation [30]. However, studies on EGT in MASLD are rare. Therefore, exploring the role and regulatory mechanisms of EGT in MASLD could provide new ideas to treat MASLD in future.

In this study, we hypothesized that EGT might ameliorate MASLD by enhancing autophagy, reducing oxidative damage and inflammation. By constructing high-fat diet (HFD)-induced mice and palmitic acid (PA)-treated AML12, it turned out that EGT ameliorated lipid metabolism disorders of the MASLD. Mechanistically, RNA sequencing and 3-MA intervention experiments suggested that EGT improved MASLD associated with the enhancement of autophagy, inhibition of oxidative damage and inflammation. Thus, this work demonstrated the potential clinical therapeutic effect and molecular mechanism of EGT on MASLD, and provided theoretical basis for future drug development in MASLD treatment.

Materials and methods

Construction of high-fat diet mouse model

5 weeks male C57BL/6J mice were purchased by Huachuang Xinnuo Technology Co., Jiangsu, China. These mice were kept in the Shandong University Laboratory Animal Center, SPF class animal house, at room temperature (22–25 ℃), 12 h dark/light cycle, and 50–60% humidity. Based on previous studies of ergothioneine [31, 32], 35 mg/kg/day was performed by water feeding. To study the dynamic pathological characteristics of the effects of EGT in HFD mice, the mice were stabilized for one week and then randomly divided into 4 groups (4 mice/cage, 2 cages/group): (1) NCD group: normal diet (SWS9102, Xiatong shengwu, Jiangsu, China) (2) NCD+EGT group: normal diet and water-fed EGT (3) HFD group: high-fat-fed (XTHF60, Xiatong shengwu, Jiangsu, China) (4) HFD+EGT group: high-fat diet and water-fed EGT. Body weights were monitored every week, intraperitoneal glucose tolerance test (IPGTT) was tested at 21 week, intraperitoneal insulin tolerance test (IPITT) was tested at 22 week, body fat was tested at 23 week, and mice were anesthetized and euthanized at 24 week, and blood and liver tissue samples were retained.

IPGTT, IPITT

IPGTT: mice were fasted for 14 h, injected intraperitoneally with 20% glucose solution (2 g anhydrous glucose/kg body weight), and tail-tip blood glucose levels were measured using a Roche blood glucose meter and glucose reagent (Accu-Chek® Performance, Roche Life Sciences, Basel, Switzerland) at fasting and 30, 60, 90, and 120 min post-injection. IPITT: mice were fasted for 8 h, injected intraperitoneally with insulin (0.75 U/kg body weight), and detection time as IPGTT.

Tissue sections staining and cell crawl staining with Oil Red O

Liver tissues were fixed in formaldehyde, embedded in paraffin, and sliced to 5 μm sections. And then, slices were baked for 1 h at 65 °C. Next, slices are put into the corresponding solution as follows: xylene for 30 min, xylene for 30 min, 100% ethanol for 5 min, 90% ethanol for 4 min, 80% ethanol for 3 min, 70% ethanol for 2 min, ddH_2O for 3 min. PBS was applied to wash sections for 3 min (repeated three times). Mouse liver paraffin sections were subsequently stained with a hematoxylin-eosin (HE) staining kit (G1005) and a periodic acid-schiff (PAS) staining kit (G1281), and liver tissue frozen sections and AML12 cells six-well plate were stained with the Oil Red O reagent (G1260, Servicebio, Wuhan, China) according to instructions. Paraffin sections were routinely deparaffinized and then subjected to immunohistochemical staining (IHC). IHC staining was performed using pH 9.0 EDTA Antigen Repair Solution (G1203, Servicebio, Wuhan, China). For IHC staining, the tissue samples were boiled at high temperature for 3 min, subjected to antigen retrieval on low temperature for 15 min, cooled to room temperature. PBS was applied to wash sections for 3 min (repeated three times). An IHC pen was used to draw a circle along the peripheral contour of the tissue, and non-specific staining blocker was applied to the tissue using a DAB kit (GK600505, Genentech, Shanghai, China). The samples were incubated at room temperature in darkness for 15 min. PBS was applied to wash sections for 3 min (repeated three times). Then, sections were incubated with goat serum working solution (Cat: ZLI9056, Zhongshan Golden Bridge, Beijing, China) for 1 h at room temperature. And then, sections were incubated with F4/80 antibody (1:10000, ab81299, Abcam, Shanghai, China) at 4 °C overnight. The following day, PBS was applied to wash sections for 3 min (repeated three times). Then, sections were incubated with goat anti-rabbit antibody (Cat: ZF-0311, Zhongshan Golden Bridge, Beijing, China) at room temperature for 1 h. PBS was applied to wash sections for 3 min (repeated three times). Next, sections were performed by DAB chromogenic and were stained with hematoxylin for 1 min. Eventually, a microscope (Olympus BX53, Tokyo, Japan) was applied to acquire images.

ELISA

The levels of alanine transaminase (ALT), aspartate transaminase (AST), total cholesterol (TC), triglyceride (TG), low-density lipoprotein cholesterol (LDL-C), high-density lipoprotein cholesterol (HDL-C), glutathione (GSH), catalase (CAT), superoxide dismutase (SOD), malondialdehyde (MDA), interlukin-1β (IL-1β) and interlukin-6 (IL-6) in mouse serum were detected according to ELISA kits instructions. ALT (Cat: C009-2-1), AST (Cat: C010-2-1), TC (Cat: A111-1-1), TG (Cat: A110-1-1), LDL-C (Cat: A113-1-1-1), HDL-C (Cat: A112-1-1), SOD (Cat: A001-1) and MDA (Cat: A003-1) assay kits were purchased from Jiancheng Biotechnology Co., Ltd, Nanjing, China. CAT (Cat: G4307) and GSH (Cat: G4305) assay kits were bought by Servicebio Technology Co., Ltd, Wuhan, China. IL-1β (Cat: RK00006) and IL-6 (Cat: RK00008) assay kits were bought by ABclonal Technology Co., Ltd, Wuhan, China.

AML12 cells culture

AML12 cells derived from the American Type Culture Collection (Rockville, MD, America). The cells culture used DMEM/F12 medium supplemented with 10% fetal bovine serum, 40 ng/mL dexamethasone, 1% penicillin-streptomycin solution, and ITS (5.5 μg/mL transferrin, 10 μg/mL insulin, and 5 μg/L sodium selenite) and incubated in 5% CO_2 and 37 °C saturated humidity (Thermo Fisher Scientific, Massachusetts, America). By assessing cell viability, 0.2 mM palmitic acid (PA) concentration was used treating the cells for 48 h (Fig. 3A and B). By testing the role of AML12 cells in gradient EGT concentrations (Fig. 3C and D), and a concentration of 0.5 mM EGT was used in vitro experiments. AML12 cells were grouped as follows: (1) Ctrl group: without EGT and PA; (2) Ctrl+EGT group: with 0.5 mM EGT and without PA; (3) PA group: with 0.2 mM PA and without EGT; (4) PA+EGT group: with 0.2 mM PA and 0.5 mM EGT. To elucidate the effects of autophagy in EGT-treated AML12, AML12 cells were treated as follows: PA and PA+EGT groups as above, PA+EGT+3MA group: pretreatment with 5 mM 3-MA for 6–8 h in advance, after which the cells were treated with 0.2 mM PA and 0.5 mM EGT for 48 h.

Cell viability assay

The cell viability assay used a Cell Counting Method-8 kit (CCK-8, BS350B, Biosharp, Beijing, China). Cells suspensions (100 μL/well, 1000–10000 cells/well) were added in 96-well plates, and the plates were at 37 °C, 5% CO_2 incubator. Then, CCK8 solution (10 μL/well) was added into the plates, which incubated in the incubator for 1–4 h. The OD values at 450 nm were tested with an enzyme marker (Varioskan Flash, Thermo Fisher Scientific, Massachusetts, America). Cell survival was calculated according to the instruction manual formula.

RNA-seq analysis

Trizol reagent (Invitrogen, Thermo Fisher Scientific, Massachusetts, America) was applied to obtain total RNA in AML12 cells. RNA-seq was performed by Qingdao Ouyi Biological Co., Ltd. Data analysis was performed using Ouyi Biological Cloud Platform (https://cloud.oebiotech.com/).

Real-time quantitative PCR (RT-qPCR)

RNA was collected using a Cell or Tissue RNA Isolation Kit (Cat: RC112, Vazyme, Nanjing, China), and reverse transcription was performed using a RT SuperMix for qPCR Kit (Cat: RC323, Vazyme, Nanjing, China). RT-qPCR was performed by utilizing a SYBR qPCR Master Mix (Cat: Q711, Vazyme, Nanjing, China) and LC480photocycler. 2-ΔΔCt method was utilized to analyse genes expression, and β-actin normalization was utilized for quantification. The gene-specific primer sequences are shown in Table 1.

Western blotting

Proteins were collected by using radioimmunoprecipitation assay (RIPA) lysis buffer (P0013B, Beyotime, Shanghai, China), and the protein concentration was tested by utilizing a bicinchoninic acid (BCA) assay (Cat: ZJ102, Epizyme, Shanghai, China). Then, proteins were subjected to sodium dodecyl sulfate-polyacrylamide gel electrophoresis. Next, proteins were incubated using anti-rabbit β-actin (AB0035, Abways, Shanghai, China), Atg5 (Cat: 10181-2-AP, Proteintech, Wuhan, China), Beclin1 (Cat:11306-1-AP, Proteintech, Wuhan, China), p62 antibodies (Cat: 18420-1-AP, Proteintech, Wuhan, China), and goat anti-rabbit IgG polyclonal secondary antibodies (Cat: ZB-2301, Zhongshan Golden Bridge, Beijing, China). Protein bands were detected by utilizing a chemiluminescence reagent (WBKLS 0050, Millipore, Massachusetts, America), and images were obtained using a chemiluminescence imaging system (Tanon Scientific Instrument Co., Ltd., Shanghai, China).

Reactive oxygen species (ROS) assay

AML12 cells were stained by using a Reactive Oxygen Species Detection kit (G1706, Servicebio, Wuhan, China). After the intervention of AML12 cells according to the experimental protocol, the supernatant was diacarded, and PBS was applied to wash cells (repeated twice), after which the DCFH-DA probe solution was diluted (1:1000) and added the plate, cells were incubated for 30 min in darkness at 37 °C, 5%CO_2 incubator. The DCFH-DA working solution was aspirated, and PBS was applied to wash plate (repeated three times). Finally, images were obtained by a confocal scanning imaging microscope (CSIM130, Sunny Group Co., Ltd., Zhejiang, China).

Apoptosis assay

Apoptotic cells were tested by utilizing Annexin V-FITC/PI Assay kit (556547, BD Biosciences, New Jersey, America). AML12 cells were digested with trypsin without ethylenediaminetetraacetic acid. Then, pre-cooled PBS was applied to wash cells, centrifugation at 1000 rpm for 5 min, cells supernatants were discarded, and cells were mixed, this washing was repeated twice. The cell precipitate was resuspended in 1×Annexin V Binging Buffer, and the cell suspension was diluted so that the cell density was approximately 1×100, 000/mL. 100 μL of the above diluted cell suspension was added in a flow tube, and 5 μL of PI and 5 μL of Annexin V-FITC staining solution were added in the flow tube. The flow tube was slightly mixed and incubated in the dark at room temperature for 15 min. Early and late apoptotic activity was tested using a Cyto FLEX flow cytometer (Beckman Coulter Inc.,

Table 1 qPCR primer sequences

Name	Forward sequences	Reverse sequences
β-actin	TGCTGTCCCTGTATGCCTCTG	TGATGTCACGCACGATTTCC
Bax	GCTACAGGGTTTCATCCAGGATC	TGCTGTCCAGTTCATCTCCAATT
Bcl2	GGATTGTGGCCTTCTTTGAGTTC	CTTCAGAGACAGCCAGGAGAAAT
Caspase7	ACTCCACGGTTCCAGGTTATTAC	ATACACGGGATCTGCTTCTTCTC
Caspase9	GCAAAGGAGCAGAGAGTAGTGAA	CGAATCCAGGGTGTATGCCATAT
Beclin1	AAACTGGACACGAGCTTCAAGAT	CCATCCTGGCGAGTTTCAATAAA
Atg5	GTTTGGCTTTGGTTGAAGGAAGA	AATTCGTCCAAACCACACATCTC
P62	CACAGGCACAGAAGACAAGAGTA	CCTGTAGATGGGTCCACTTCTTT
FASN	CCTTCCGTCACTTCCAGTTAGAG	AAGTTCAGTGAGGCGTAGTAGAC
CPT1α	GCAAATGATGTGGACCTGCATTC	AGAACTTGCCCATGTCCTTGTAA
PPARα	TTCCCTGTTTGTGGCTGCTATAA	CTTCTTGATGACCTGTACGAGCT
ApoB	CCACCAAACTGCTCTTCCAAATG	GGTTCCCGTGTTCCAATCAAATT
IL-6	AACCGCTATGAAGTTCCTCTCTG	TGGTATCCTCTGTGAAGTCTCCT
IL-10	CAGAGAAGCATGGCCCAGAAATC	GCTCCACTGCCTTGCTCTTATTT
IL-1β	CAGCACATCAACAAGAGCTTCAG	GAGGATGGGCTCTTCTTCAAAGA
TNF-α	GCCTCCCTCTCATCAGTTCTATG	ACCTGGGAGTAGACAAGGTACAA
SOD3	GCTACTGTGTTCCTGCCTGCT	ATCTCCGTGACCTTGGCGTA
CAT	CAGGCTCTTCTGGACAAGTACAA	GAGAATCCATCCAGCGTTGATTAC
GPX4	CTGCTCTTCCAGAGGTCCTG	GAGGTGTCCACCAGAGAAGC

California, America), and the apoptosis data were analysed by Flowjo.

Dual-energy X-ray body fat content test

Body fat was detected using a dual-energy X-ray bone densitometer (GE Lunar DPX Prodigy, GE, Boston, America). First, the "Prodigy" software in the computer connected to the bone densitometer was opened, a new testing object was crested, and the tested object information (including number, birth date, weight, sex, and species) was input. Second, the "Small animal whole body test" was selected, and each anesthetized mouse was fixed so that its nose was at the center of the red positioning mark in the bone densitometer examination table. Then, the detection range was selected according to the size of mouse (usually length: 15 cm; width: 10 cm), and the "measure" option was selected. Finally, the body fat content data were saved and recorded.

Data analysis

All experimental data were analysed with GraphPad Prism 9.0. The results of experimental data were presented as mean±standard deviation (Mean±SD). Comparisons of multiple groups data were performed using one-way ANOVA and Tukey's adjusted test. P□0.05 indicate statistical differences.

Results

Ergothioneine ameliorated lipid metabolism and liver impairment in HFD mice

To research the effects of ergothioneine in MASLD, this study constructed high-fat mice model, and mice were treated with EGT or without EGT according to Fig. 1A. The body weight, area under the curve (AUC) of IPGTT and IPITT in HFD group were increased compared to NCD group, indicating that HFD group had significant insulin resistance and impairments of glucose tolerance (Fig. 1B-D). However, body weights were decreased (Fig. 1B) and insulin sensitivity and glucose tolerance were enhanced in HFD+EGT group (Fig. 1C and D). Furthermore, serum levels of ALT and AST were elevated in HFD group as opposed to NCD group (Fig. 1E and F). Dual-energy X-ray absorption photometry revealed that the body fat of HFD group was added in comparison with NCD group (Fig. 1G). Nevertheless, liver function and body fat in HFD+EGT group were decreased compared to HFD group (Fig. 1E-G). Therefore, the above findings implied that ergothioneine could reduce body weight, insulin resistance, hepatic function impairment, and body fat in high-fat diet mice.

Ergothioneine ameliorated hepatic structural damage, hyperlipidemia, oxidative stress, autophagy and inflammation in HFD mice

Paraffin sections of mouse livers were stained histologically (Fig. 2A). HE staining revealed that NCD group was normal and that the structure of liver lobules was clear. The number of liver steatosis vacuoles rose in HFD group but reduced in HFD+EGT group. PAS staining revealed that liver glycogen deposition rose in HFD group, while reduced in HFD+EGT group. Oil Red O staining revealed that there was few lipid droplet deposition in NCD group, whereas there were many lipid droplets in HFD group. However, lipid droplets were reduced in HFD+EGT group. F4/80 (macrophage activation marker) of IHC staining revealed that liver macrophages in HFD group were activated, but macrophages activation were attenuated in the HFD+EGT group. Serum lipid assays showed that TC, TG, and LDL-C levels were rose (Fig. 2B-D) and HDL-C were reduced (Fig. 2E) in HFD group, indicating that HFD group had significant hyperlipidemia. Nevertheless, the above lipid levels were improved in HFD+EGT group (Fig. 2B-E). ELISA results indicated that antioxidant enzymes GSH, SOD, and CAT levels were decreased (Fig. 2F-H), and the levels of MDA (Fig. 2I) and inflammatory indicators IL-1β and IL-6 were rose in HFD group (Fig. 2J and K). However, the above inflammation and oxidative stress indicators were improved in HFD+EGT group (Fig. 2F-K). Moreover, compared to HFD group, the mRNA and protein levels of Atg5, Beclin1, and p62 were improved in HFD+EGT group (Fig. S1I-L). The above results suggested that ergothioneine ameliorated liver structural damage, hyperlipidemia, oxidative stress, autophagy and inflammation in HFD mice.

Ergothioneine attenuated PA-induced lipid metabolism impairment in AML12 cells

PA stimulation of AML12 cells is a classical in vitro lipotoxicity model. The CCK8 kit assayed the cell viability at gradient PA concentrations and for different durations (Fig. 3A). Oil Red O was used assess the lipid deposition status of AML12 treated with gradient PA concentrations for 48 h (Fig. 3B). For the combination of cell viability and lipid deposition status results, a PA concentration of 0.2 mM for 48 h was the optimal condition for lipotoxicity model in vitro. Then, different concentrations of ergothioneine (0–2 mM) were used to treat AML12 cells. CCK8 and Oil Red O tests showed that ergothioneine improved cell viability (Fig. 3C) and lipid deposition (Fig. 3D). Combining the above experimental results, this study ultimately selected 0.5 mM EGT to treat AML12.

Compared to Ctrl group, the mRNA level of FASN (a fatty acid synthase) was increased (Fig. 3E), and the mRNA levels of ApoB (apolipoprotein B gene, a lipid

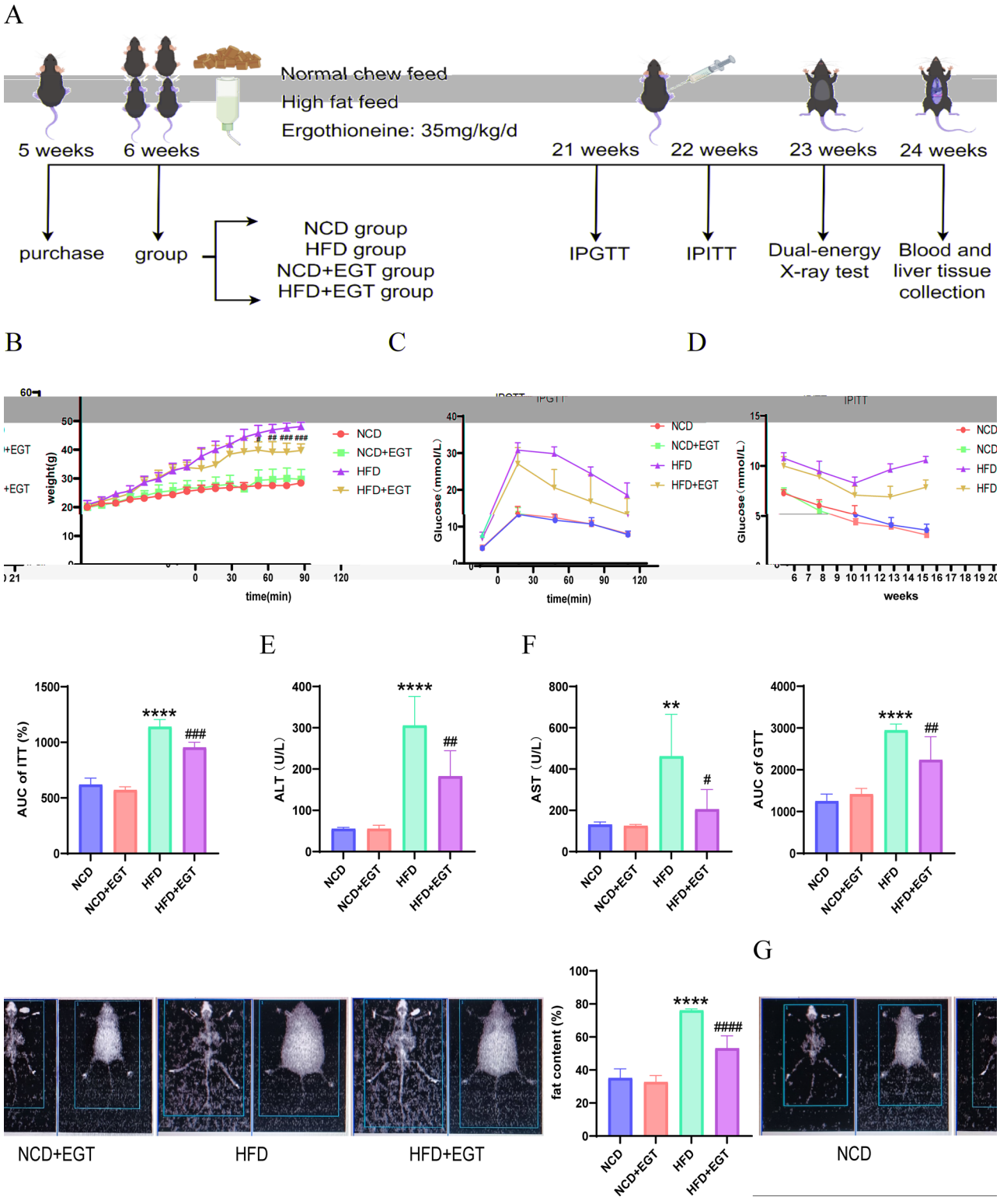

Fig. 1 Ergothioneine ameliorated lipid metabolism and liver impairment in HFD mice. (**A**) Graph of the experimental design for mice. (**B**) Body weight change curve of mice. The plot of the statistical analysis results and the (AUC) of IPGTT (**C**) and IPITT (**D**). Serum levels of ALT (**E**) and AST (**F**) in mice. (**G**) Graph of statistical analysis of mouse body fat and percentage by dual-energy X-ray absorption photometry. $n = 5$. ** $P < 0.01$, **** $P < 0.0001$ HFD vs. NCD; $^{\#}P < 0.05$, $^{\#\#}P < 0.01$, $^{\#\#\#}P < 0.001$, $^{\#\#\#\#}P < 0.0001$ HFD + EGT vs. HFD

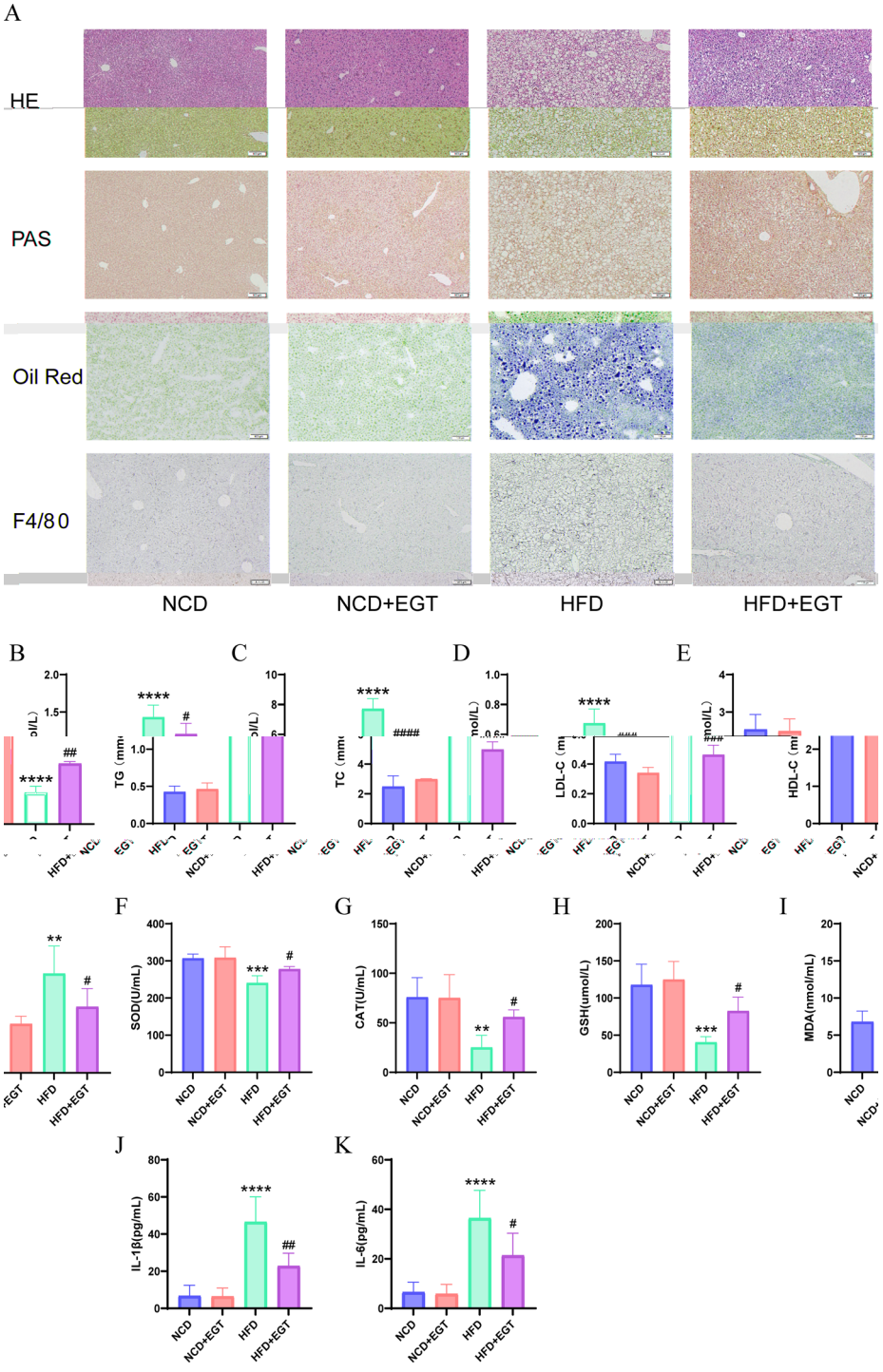

Fig. 2 Ergothioneine ameliorated hepatic structural damage, hyperlipidemia, oxidative damage, and inflammation in HFD mice. (**A**) HE, PAS, Oil Red, and IHC (F4/80) staining. Bar = 100 μm. Serum levels of TG (**B**), TC (**C**), LDL-C (**D**) and HDL-C (**E**) in mice. ELISA kits detected serum levels of SOD (**F**), CAT (**G**), GSH (**H**), MDA (**I**), IL-1β (**J**) and IL-6 (**K**) in mice. $n = 5$. ** $P < 0.01$, *** $P < 0.001$, **** $P < 0.0001$ HFD vs. NCD; $^{\#}P < 0.05$, $^{\#\#}P < 0.01$, $^{\#\#\#}P < 0.001$, $^{\#\#\#\#}P < 0.0001$ HFD + EGT vs. HFD

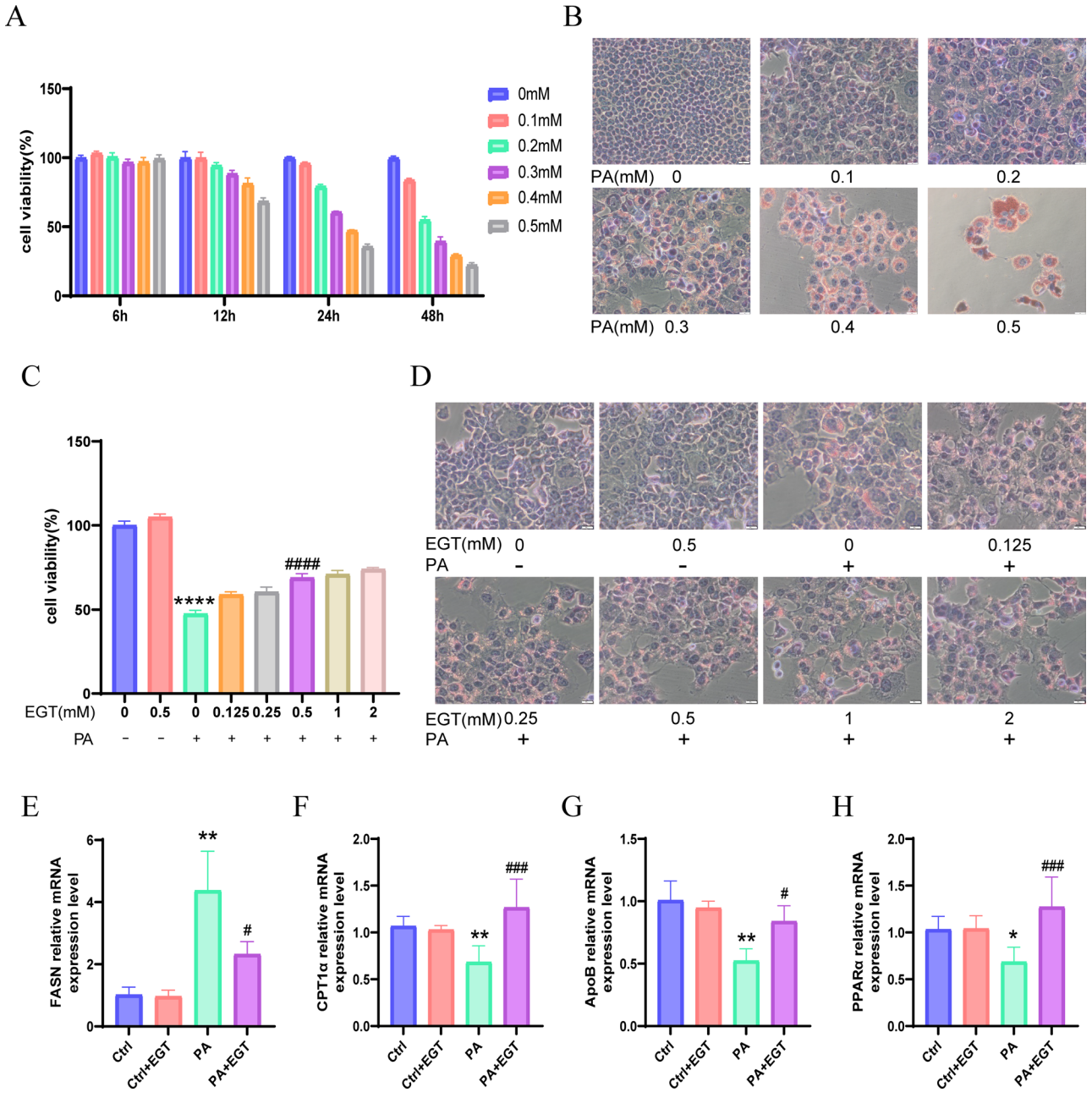

Fig. 3 Ergothioneine attenuated PA-induced lipid metabolism impairment in AML12. (**A**) Percentage of AML12 cells viability detected by CCK8. (**B**) Status of AML12 lipid deposition detected by Oil Red. (**C**) Percentage of cell viability in AML12 cells intervened by ergothioneine at different concentrations detected by CCK8. (**D**) Status of AML12 lipid deposition intervened by ergothioneine at different concentrations detected by Oil Red. qPCR detected FASN (**E**), CPT1α (**F**), ApoB (**G**) and PPARα (**H**) mRNA expression levels in AML12 cells. mM: mmol/L, bar:20 μm, $n=3$. * $P<0.05$, ** $P<0.01$, **** $P<0.0001$ PA vs. Ctrl; $^{\#}P<0.05$. $^{\#\#\#}P<0.001$, $^{\#\#\#\#}P<0.0001$ PA + EGT vs. PA

transport-related molecule) and PPARα (peroxisome proliferator-activated receptor α, involved in fatty acid oxidation) and CPT1α (carnitine palmitoyltransferase-1α, a fatty acid oxidation-related molecule) were decreased in PA group (Fig. 3F-H). However, these genes mRNA levels were improved in PA+EGT group (Fig. 3E-H). The above results suggested that ergothioneine attenuated lipid deposition and lipid metabolism impairment in PA-treated AML12 cells.

RNA-seq analysis revealed that ergothioneine protected AML12 cells by improving autophagy, apoptosis, and oxidative damage

To elucidate the effects of ergothioneine in AML12 cells, RNA-seq was performed in the Ctrl, PA, and PA+EGT

groups of AML12 cells. The sequencing results revealed that principal component analysis (PCA) distinguished the PA group samples from PA + EGT group (Fig. 4A). The cluster analysis of the PA + EGT group vs. the PA group clearly showed that differential expression was significant after EGT intervention (Fig. 4B). A volcano plot was constructed and revealed 6458 differential expressed genes, with 3375 genes downregulated and 3058 genes upregulated in PA + EGT group in contrast to PA group (Fig. 4C). Cellular inflammation and immune responses

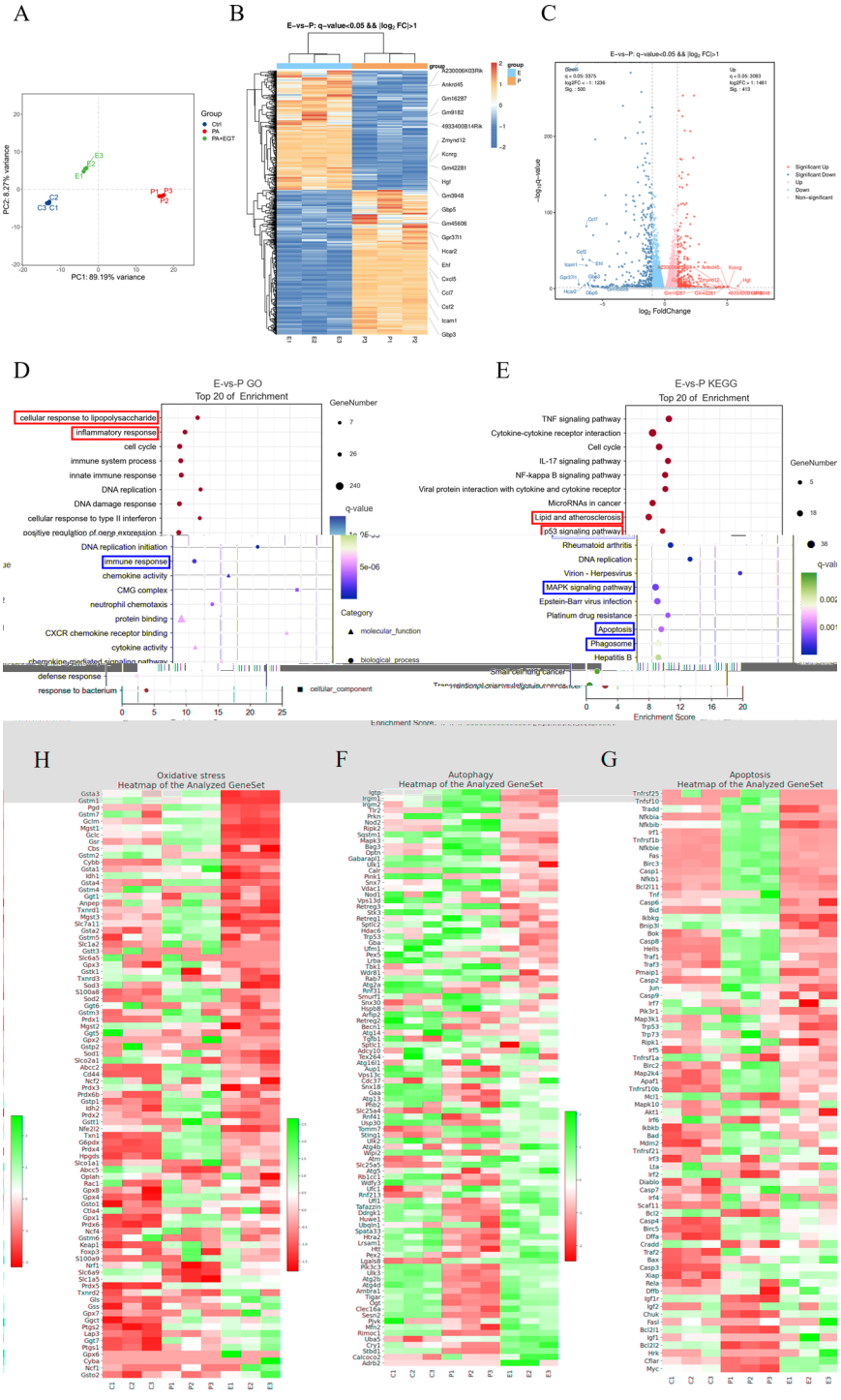

Fig. 4 Analyses of transcriptomic differences ergothioneine-treated AML12 cells. (**A**) Principal component analysis (PCA) of RNA-seq in AML12. (**B-E**) Difference analysis of PA + EGT vs. PA sequencing results. (**B**) Cluster analysis. (**C**) Volcano plots. GO (**D**) and KEGG (**E**) enrichment analysis. (**F-H**) Heatmap of GSEA analysis. Heatmap of autophagy (**F**), apoptosis (**G**) and oxidative stress (**H**) related gene expression profiles. C: Ctrl, P: PA, E: PA + EGT, $n = 3$

were enriched, as shown by the top 20 GO enrichment results of the PA+EGT group vs. the PA group (Fig. 4D). Analysis of the top 20 enriched KEGG pathway for the PA+EGT group vs. the PA group revealed that signaling pathways related to apoptosis, lipid metabolism, phagolysosomes, p53, and MAPK were enriched (Fig. 4E). Compared to Ctrl group, PA group genes involved in autophagy (Fig. 4F), apoptosis (Fig. 4G), and oxidative stress (Fig. 4H) pathways presented significant changes in gene expression, however, these changes were reduced in the PA+EGT group. Thus, RNA-seq analysis showed that ergothioneine protected AML12 cells by autophagy, apoptosis, and oxidative stress pathways.

Ergothioneine attenuated oxidative stress injury and inflammation to ameliorate PA-induced lipotoxic injury in AML12

To verify the effects of EGT improving oxidative damage and inflammation in PA-induced AML12 cells. Based on ROS fluorescent probe assay, in contrast to Ctrl group, ROS level of PA group was added. However, ROS level was declined in PA+EGT group compare to PA group (Fig. 5A). qPCR assays of antioxidant enzymes demonstrated that CAT, SOD3, and GPX4 mRNA levels were declined compared to Ctrl group, but antioxidant enzymes levels were enhanced in PA+EGT group (Fig. 5B-D). qPCR tests indicated that proinflammatory mediators IL-1β, IL-6, and TNF-α mRNA levels were added (Fig. 5E-G) and anti-inflammatory factor interlukin-10 (IL-10) mRNA levels were reduced in PA group compared to Ctrl group (Fig. 5H). ELISA revealed that cell supernatant levels of IL-1β and IL-6 were added in PA group in comparison with Ctrl group (Fig. 5I and J). However, the mRNA and cell supernatant levels of these inflammatory indicators were ameliorated in PA+EGT group (Fig. 5E-J). The above results suggested that ergothioneine attenuated oxidative stress injury and inflammation to ameliorate PA-induced lipotoxic injury in AML12.

Ergothioneine attenuated apoptosis and promoted autophagy to ameliorate PA-induced lipotoxic injury in AML12

GSEA analysis of RNA sequencing revealed that EGT enhanced autophagy and attenuated apoptosis. To further confirm the role of EGT in improving autophagy and apoptosis in AML12 cells, flow cytometry and qPCR were applied to test the percentage of AML12 apoptosis and Bax, Bcl2, caspase7 and caspase9 mRNA levels. These figures presented that the percentage of apoptosis and mRNA levels of related molecules were added in PA group, but were reduced in PA+EGT group (Fig. 6A-F). qPCR detection of autophagy levels revealed that autophagy was suppressed in PA group with added p62 expression and decreased Beclin1 and Atg5 expression (Fig. 6G-J). However, the expression levels of these autophagy-regulated genes were significantly improved in PA+EGT group (Fig. 6G-J). These findings suggested that ergothioneine could attenuate apoptosis and promote autophagy to ameliorate PA-induced AML12 lipotoxicity injury.

3-MA blocked the protective role of ergothioneine in AML12

To further confirm the mechanism of EGT protecting AML12, AML12 cells were pretreated with 3-MA (a common autophagy inhibitor) for 6–8 h, followed by PA and ergothioneine intervention. qPCR tests and Oil Red O staining showed that 3-MA aggravated lipid deposition (Fig. 7A), upregulated FASN mRNA expression (Fig. 7B), and downregulated ApoB and PPARα mRNA expression levels (Fig. 7C and D). Besides, 3-MA added ROS level (Fig. 7E) and reduced mRNA levels of the antioxidant enzymes SOD3, CAT, and GPX4 (Fig. 7F-H). ELISA findings revealed that 3-MA increased levels of IL-1βand IL-6 in AML12 cell supernatant (Fig. 7I and J). Flow cytometry and qPCR results indicated that 3-MA increased the percentage of apoptosis (Fig. 7K), and upregulated the mRNA levels of Bax/Bcl2 (Fig. 7L), caspase7 (Fig. 7M) and caspase9 (Fig. 7N). The above results indicated that 3-MA blocked ameliorative effects of ergothioneine in lipid metabolism, apoptosis, oxidative damage, and inflammation in AML12 cells.

Discussion

Some studies on MASLD have shown that fat accumulation, IR, oxidative damage, and inflammation in liver are major contributors to the development of MASLD [33, 34]. Therefore, reductions in hepatic fat accumulation, the inflammation and oxidative damage are beneficial for the prevention and treatment of MASLD. Currently, some studies have demonstrated that EGT has preventive or therapeutic potential for a range of oxidative stress-related diseases [35]. Based on the limitations of therapeutic drugs for MASLD, the non-toxic nature of ergothioneine, and the anti-inflammatory and antioxidant cytoprotective roles, this work concentrated on the protective role of EGT in MASLD through autophagy and the related mechanisms by constructing a high-fat model in vivo and in vitro.

In this work, the MASLD models were constructed through high-fat diet feeding C57BL/6J mice. Because MASLD is a chronic metabolic disease, these mice were treated with high-fat diet and ergothioneine (35 mg/kg/d) from week 6 until week 24. The dosage used was described in previous studies [31, 32], and 35 mg/kg/d fully saturated the intracellular accumulation and metabolism of EGT in mice [32]. Additionally, the

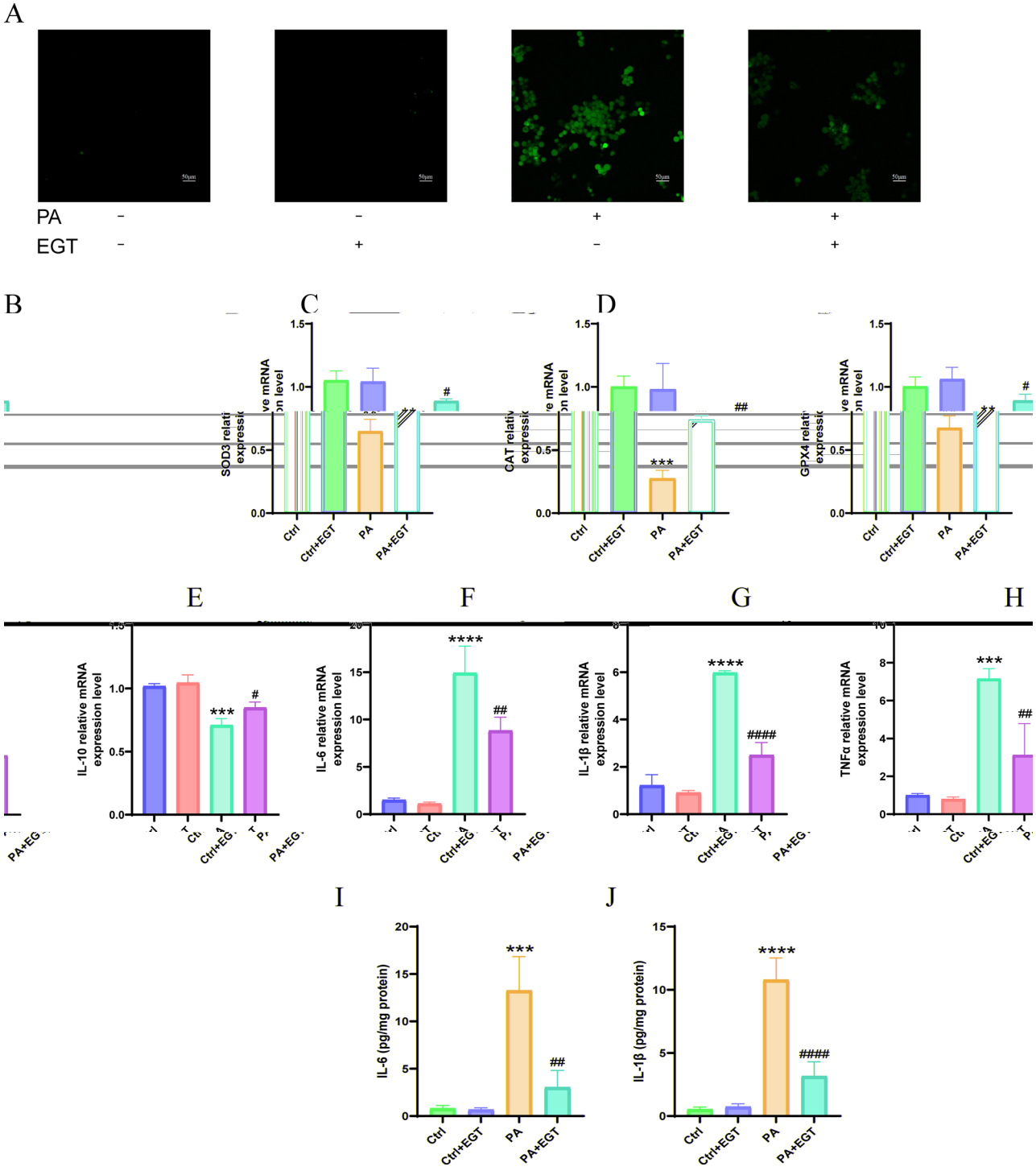

Fig. 5 Ergothioneine attenuated oxidative stress injury and inflammation to ameliorate PA-induced lipotoxic injury in AML12. (**A**) ROS assay. qPCR detected SOD3 (**B**), CAT (**C**), GPX4 (**D**), IL-6 (**E**), IL-1β (**F**), TNF-α (**G**) and IL-10 (**H**) mRNA expression levels. ELISA detected IL-6 (**I**) and IL-1β (**J**) levels in AML12 cell supernatant. Bar:50 μm, $n = 3$. ** $P < 0.01$, *** $P < 0.001$, **** $P < 0.0001$ PA vs. Ctrl; $^{\#}P < 0.05$, $^{\#\#}P < 0.01$, $^{\#\#\#\#}P < 0.0001$ PA + EGT vs. PA

safety of this intervention has been intensively investigated, EGT has been approved as a nutritional supplement by the European Food Safety Authority and the Food and Drug Administration [36]. Moreover, there are no developmental abnormalities and death in mice in the EGT intervention group with weekly monitoring, thus confirming the safety of EGT. In vivo experiments revealed that EGT decreased body weight and insulin resistance in HFD mice and significantly improved body fat content, liver function, and lipid metabolism genes

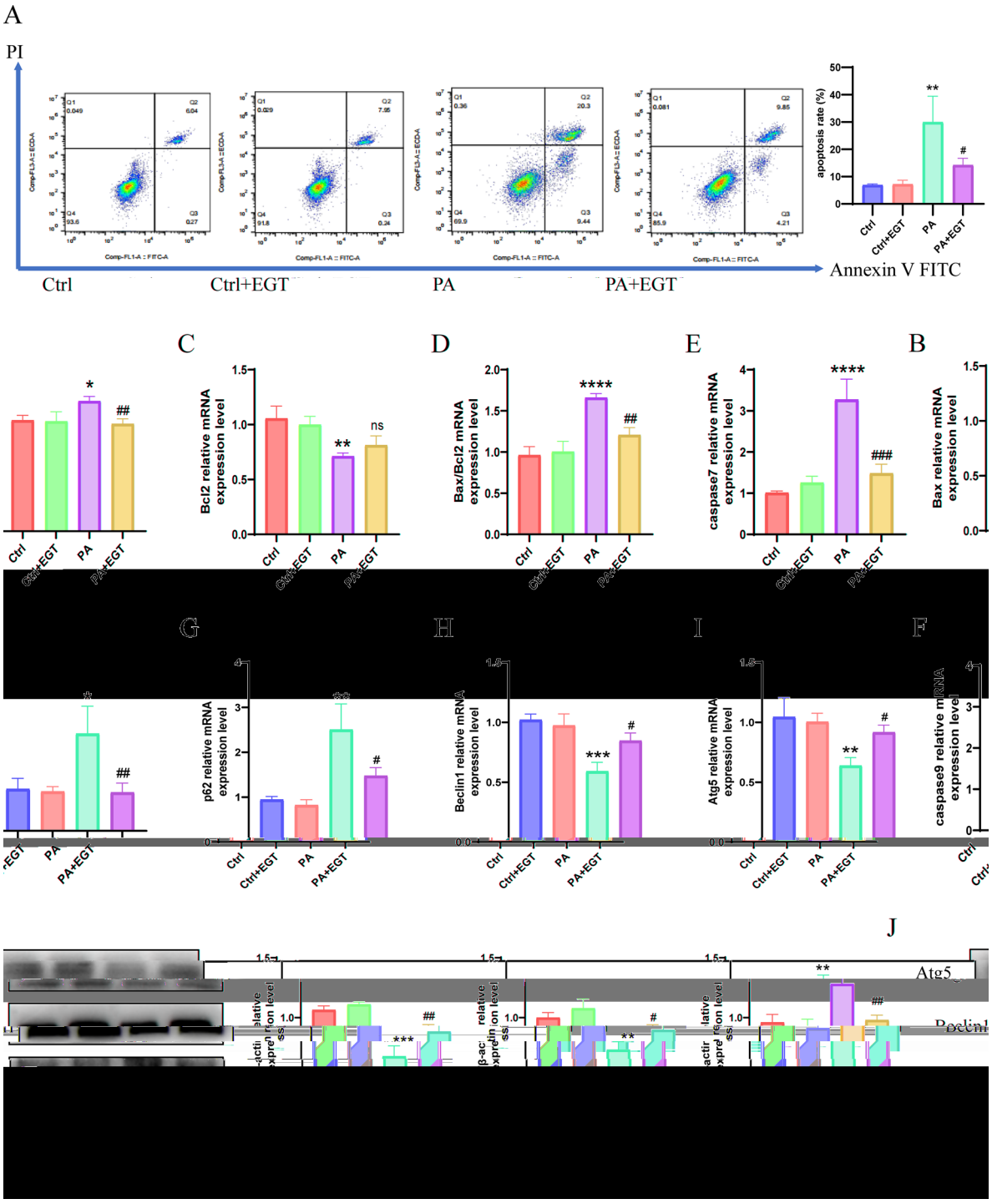

Fig.6 Ergothioneine attenuated apoptosis and promoted autophagy to ameliorate PA-induced lipotoxic injury in AML12. (**A**) Flow cytometry detection of apoptosis level and statistical analysis graph. qPCR detected Bax (**B**), Bcl2 (**C**), Bax/Bcl2 (**D**), caspase7 (**E**), caspase9 (**F**), p62 (**G**), Beclin1 (**H**) and Atg5 (**I**) mRNA expression levels in AML12 cells. (**J**) Western blotting detected Atg5, Beclin1, and p62 protein expression levels and statistic plots in AML12. $n=3$. * $P<0.05$, ** $P<0.01$, *** $P<0.001$, **** $P<0.0001$ PA vs. Ctrl; ns $\geqq 0.05$, $^{\#}P<0.05$, $^{\#\#}P<0.01$, $^{\#\#\#}P<0.001$ PA + EGT vs. PA

expression levels (Fig. S1E-H), as well as reduced liver ballooning degeneration, lipid deposition, and glycogen accumulation in the EGT-intervened group of HFD-fed mice; rather, EGT markedly alleviated inflammation and enhanced the levels of antioxidant enzymes in HFD mice. These experiments revealed that EGT might improve lipid metabolism dysfunction in HFD mice, reflecting the protective effect of EGT on the livers of these mice.

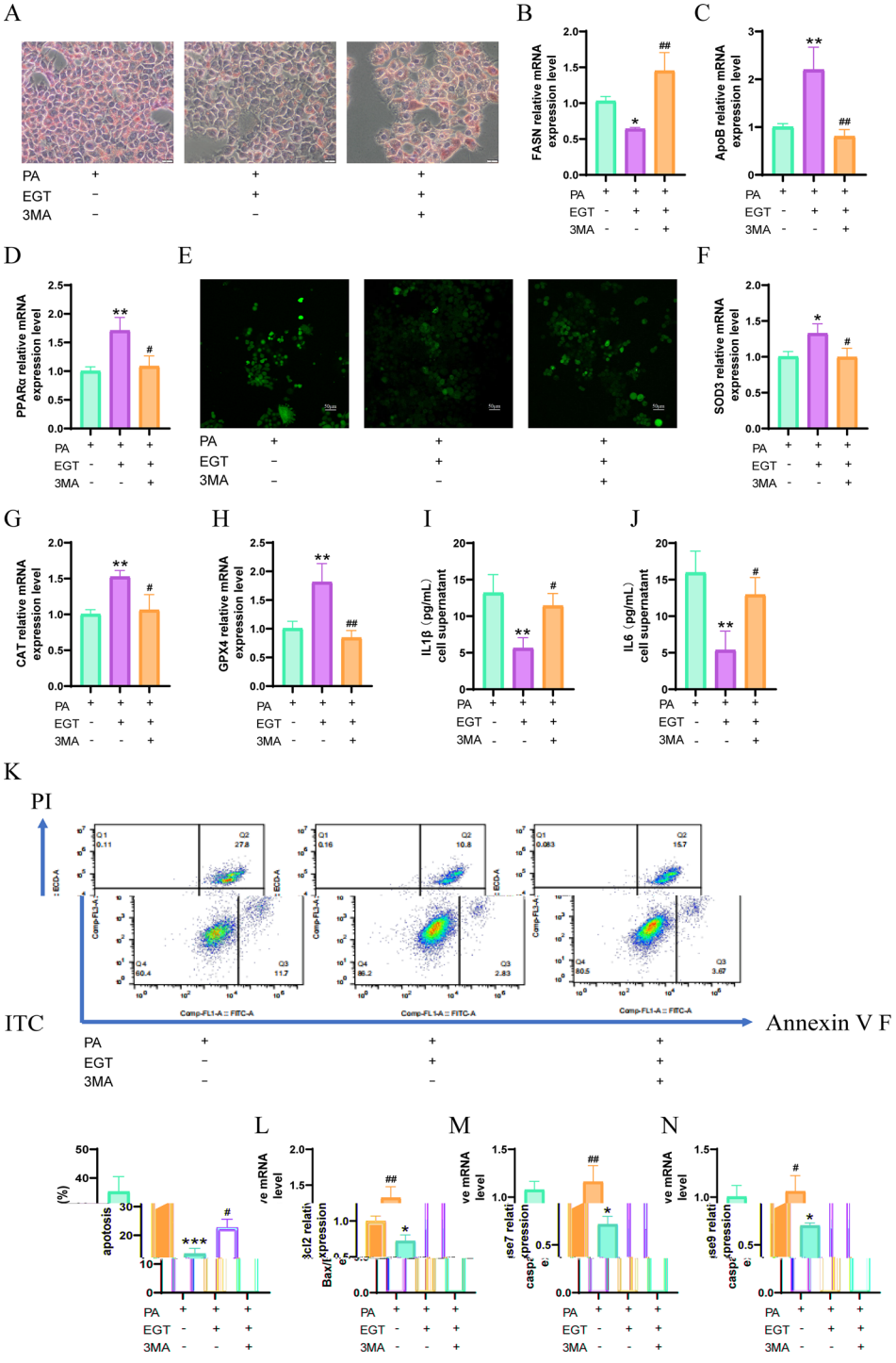

Fig. 7 3-MA blocked the protective role of ergothioneine in AML12. (**A**) Oil Red O assay for lipid deposition. Bar:20 μm. qPCR detected FASN (**B**), ApoB (**C**) and PPARα (**D**) mRNA expression levels in AML12 cells. (**E**) ROS assay. Bar:50 μm. qPCR detected SOD3 (**F**), CAT (**G**) and GPX4 (**H**) mRNA expression levels in AML12. ELISA detected IL-1β (**I**) and IL-6 (**J**) levels in AML12 cell supernatant. (**K**) Flow cytometry detected the rate of apoptosis and statistical analysis of the data in the graphs. qPCR detected Bax/Bcl2 (**L**), caspase7 (**M**) and caspase9 (**N**) mRNA expression levels in AML12 cells. $n = 3$. * $P < 0.05$, ** $P < 0.01$, *** $P < 0.001$ PA + EGT vs. PA; $^{\#}P < 0.05$, $^{\#\#}P < 0.01$ PA + EGT + 3MA vs. PA + EGT

For the in vitro experiments, the saturated fatty acid PA, which is widely used in in vitro cell line lipotoxicity studies, induced lipid metabolism disorders in AML12 cells [37]. In accordance with previous studies [38, 39], Oil Red O staining and CCK8 findings demonstrated that 0.2 mM PA was appropriate to treat AML12 cells for 48 h to construct in vitro high-fat models. The expression levels of relevant lipid metabolism molecules FASN, CPT1α, PPARα, and ApoB were detected, and it was found that EGT was able to significantly improve PA-induced lipid metabolism dysfunction.

The above in vitro and *vivo* experiments demonstrated that EGT could significantly improve the hepatic lipid metabolism function. To elucidate the related mechanism, RNA-seq was performed in AML12 cells. GO and KEGG pathway enrichment analysis revealed that the cellular inflammation, apoptosis, lipid metabolism, phagosomes, MAPK, and p53 signaling pathways were enriched after EGT intervention. GSEA revealed that autophagy was increased and that apoptosis and oxidative stress were inhibited after EGT intervention. As autophagy and apoptosis regulate each other, they worked together to regulate homeostasis and cell death in the organism [40]. In most instances, promoting autophagy inhibited the activation of apoptosis and promoted cell survival [41]. Moreover, autophagy was involved in many cellular physiological processes and stress responses, such as the regulation of oxidative damage and inflammation [42, 43]. Thus, the study speculated that EGT might play a protective role via promoting autophagy and attenuating apoptosis and oxidative stress in MASLD.

To test this hypothesis, this study tested the autophagy, inflammation and oxidative damage levels in vitro and in vivo. Previous studies verified that MAPK and Erk1 expression levels were reduced, and mTOR was inhibited, but ULK1 expression was promoted, resulting in the activation of autophagy [40]. This study also confirmed this result in AML12 cells (Fig. S1A-D). In vitro and in vivo findings indicated that EGT could significantly upregulate Beclin1 (A well-established regulator of PI3K autophagy complex formation [44, 45]) and Atg5 (A key component regulating the formation of the autophagosome [46, 47]) expression, and downregulate p62 (An ubiquitin-binding adapter protein associated with impaired autophagic flux [17, 48]) expression, and restored the suppressed autophagic flux in HFD group. EGT also downregulated the mRNA expression of Bax/Bcl2, caspase7 and caspase9, and reduced the number of apoptotic cells, and attenuated PA-induced apoptosis. Moreover, EGT added the expression of SOD3, CAT, and GPX4, and attenuated the ROS levels and the expression of inflammatory indicators IL-1β, IL-6, IL-10, and TNF-α, which attenuated PA or HFD-induced liver injury. Then, by using the autophagy inhibitor 3-MA to intervene AML12 cells, it turned out that 3-MA blocked the ameliorative effects of EGT on lipid deposition, apoptosis, oxidative damage, and inflammation in AML12. Collectively, this study confirmed that autophagy is essential in the ameliorative effects of EGT on MASLD, which may inhibit apoptosis, oxidative stress, and inflammation on MASLD.

Study strengths and limitations

The current study has the following strengths. To start with, the study indicated for the first time that EGT ameliorates the development of MASLD. In addition, further studies revealed that EGT may ameliorate liver injury in MASLD via enhancing autophagy, inhibiting oxidative damage and inflammation, providing new insights and theoretical basis into the clinical drug treatment of MASLD. However, there are some limitations in this study. In the first place, in vitro intervention experiments using RNA sequencing and the autophagy inhibitor 3-MA demonstrated that autophagy is a crucial molecule in EGT protection of MASLD, but in vivo experiments are requested to further investigate the effect of autophagy in this. Furthermore, although this study enriched the p53 and MAPK signaling pathways related to the upstream of autophagy, and also detected that EGT depressed the mRNA expression of MAPK and Erk1, whereas these results could not prove the specific molecular targets of action of EGT in regulating autophagy, and further studies are required to verify the specific molecular mechanisms in which EGT improves MASLD.

Conclusion

This study demonstrates that ergothioneine ameliorates metabolic dysfunction-associated steatotic liver disease by promoting autophagy to attenuate lipid accumulation, oxidative stress, inflammatory response and apoptosis (Fig. 8). This work provides a new idea into the clinical treatment and dietary care of MASLD. In the future, ergothioneine is likely to be used as a dietary supplement or drug to slow the progression of MASLD and ameliorate the lipotoxic damage to the liver in patients with MASLD.

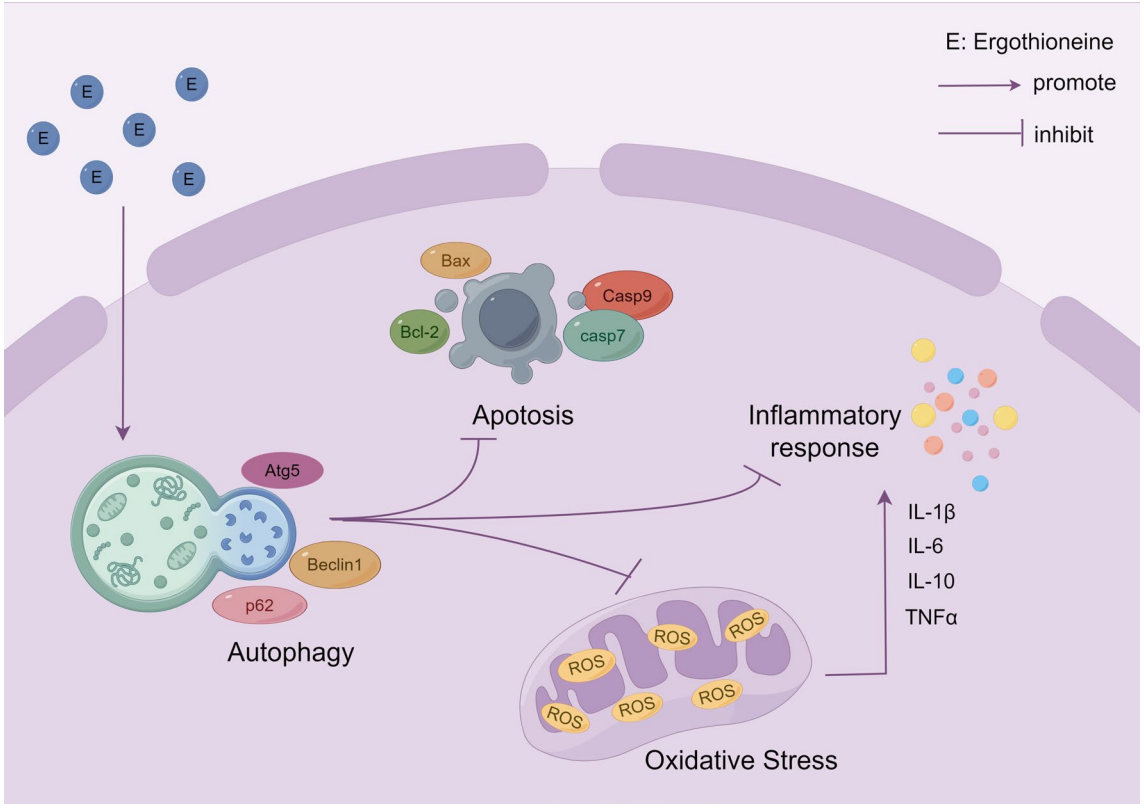

Fig. 8 Mechanism of action of ergothioneine. Ergothioneine ameliorated metabolic dysfunction-associated steatotic liver disease by enhancing autophagy, inhibiting oxidative damage and inflammation

Abbreviations

ALT	Alanine Transaminase
AST	Aspartate Transaminase
BCA	Bicinchoninic Acid
CAT	Catalase
EGT	Ergothioneine
GSH	Glutathione
HDL-C	High-Density Lipoprotein Cholesterol
HE	Hematoxylin-Eosin
IHC	Immunohistochemical Staining
IL-1β	Interlukin-1β;
IL-6	Interlukin-6
IL-10	Interlukin-10
IPGTT	Intraperitoneal Glucose Tolerance Test
IPITT	Intraperitoneal Insulin Tolerance Test
LDL-C	Low-density Lipoprotein Cholesterol
MASLD	Metabolic Dysfunction-Associated Steatotic Liver Disease
MDA	Malondialdehyde
PA	Palmitic Acid
PAS	Periodic Acid-Schiff
RIPA	Radio Immunoprecipitation Assay
ROS	Reactive Oxygen Species
SOD	Superoxide Dismutase
TC	Total Cholesterol
TG	Triglyceride
TNF-α	Tumor Necrosis Factorα;
3-MA	3-Methyladenine

Supplementary Information

The online version contains supplementary material available at https://doi.org/10.1186/s12944-024-02382-9.

Supplementary Material 1

Supplementary Material 2

Supplementary Material 3

Supplementary Material 4

Acknowledgements

We thank the Endocrine Laboratory of Qilu Hospital, Shandong University for providing platform support, and all authors for their help in data analysis and experimental procedures.

Author contributions

Xiaoyu Lv conducted the study, analyzed the data, and drafted the manuscript. Chenyu Nie, Yihan Shi, and Qincheng Qiao coordinated the research. Jing Gao, Ying Zou, Jingwen Yang, and Li Chen revised the manuscript. Xinguo Hou originated the idea. The final manuscript was reviewed and approved by all authors.

Funding

This work was supported by the National Natural Science Foundation of China (Grant NO.82270845) and Double First Class University Plan (Grant NO.26010162914001). Besides, this study was also funded by the National Key Research and Development Program of China (Grant NO.2023YFA1801100, Grant NO.2023YFA1801104) and the Taishan Scholars Program of Shandong Province (Grant No. tstp20231250).

Data availability

No datasets were generated or analysed during the current study.

Declarations

Ethics approval and consent to participate
All experiments and treatments in mice were in accordance with the International Guidelines for the Use of Laboratory Animals. The animal experiments were approved by the Laboratory Animal Ethics Committee of Shandong University (approval number: 24009).

Competing interests
The authors declare no competing interests.

Received: 16 April 2024 / Accepted: 18 November 2024
Published online: 28 November 2024

References

1. Rinella ME, Lazarus JV, Ratziu V, Francque SM, Sanyal AJ, Kanwal F, Romero D, Abdelmalek MF, Anstee QM, Arab JP, et al. A multisociety Delphi consensus statement on new fatty liver disease nomenclature. J Hepatol. 2023;79:1542–56.
2. Younossi ZM, Stepanova M, Younossi Y, Golabi P, Mishra A, Rafiq N, Henry L. Epidemiology of chronic liver diseases in the USA in the past three decades. Gut. 2020;69:564–8.
3. Argo CK, Caldwell SH. Epidemiology and natural history of non-alcoholic steatohepatitis. Clin Liver Dis. 2009;13:511–31.
4. Starley BQ, Calcagno CJ, Harrison SA. Nonalcoholic fatty liver disease and hepatocellular carcinoma: a weighty connection. Hepatology. 2010;51:1820–32.
5. Wong RJ, Aguilar M, Cheung R, Perumpail RB, Harrison SA, Younossi ZM, Ahmed A. Nonalcoholic steatohepatitis is the second leading etiology of liver disease among adults awaiting liver transplantation in the United States. Gastroenterology. 2015;148:547–55.
6. Adams LA, Anstee QM, Tilg H, Targher G. Non-alcoholic fatty liver disease and its relationship with cardiovascular disease and other extrahepatic diseases. Gut. 2017;66:1138–53.
7. Younossi ZM. Non-alcoholic fatty liver disease - A global public health perspective. J Hepatol. 2019;70:531–44.
8. Younossi ZM, Koenig AB, Abdelatif D, Fazel Y, Henry L, Wymer M. Global epidemiology of nonalcoholic fatty liver disease-Meta-analytic assessment of prevalence, incidence, and outcomes. Hepatology. 2016;64:73–84.
9. Chan WK, Chuah KH, Rajaram RB, Lim LL, Ratnasingam J, Vethakkan SR. Metabolic dysfunction-Associated Steatotic Liver Disease (MASLD): a state-of-the-art review. J Obes Metab Syndr. 2023;32:197–213.
10. Targher G, Byrne CD, Tilg H. MASLD: a systemic metabolic disorder with cardiovascular and malignant complications. Gut. 2024;73:691–702.
11. Shulman GI. Cellular mechanisms of insulin resistance. J Clin Invest. 2000;106:171–6.
12. Tarantino G, Finelli C. What about non-alcoholic fatty liver disease as a new criterion to define metabolic syndrome? World J Gastroenterol. 2013;19:3375–84.
13. Jou J, Choi SS, Diehl AM. Mechanisms of disease progression in nonalcoholic fatty liver disease. Semin Liver Dis. 2008;28:370–9.
14. Mizushima N, Komatsu M. Autophagy: renovation of cells and tissues. Cell. 2011;147:728–41.
15. Xie Z, Klionsky DJ. Autophagosome formation: core machinery and adaptations. Nat Cell Biol. 2007;9:1102–9.
16. Czaja MJ, Ding WX, Donohue TM Jr., Friedman SL, Kim JS, Komatsu M, Lemasters JJ, Lemoine A, Lin JD, Ou JH, et al. Functions of autophagy in normal and diseased liver. Autophagy. 2013;9:1131–58.
17. Sadeghi A, Niknam M, Momeni-Moghaddam MA, Shabani M, Aria H, Bastin A, Teimouri M, Meshkani R, Akbari H. Crosstalk between autophagy and insulin resistance: evidence from different tissues. Eur J Med Res. 2023;28:456.
18. Lamark T, Johansen T. Aggrephagy: selective disposal of protein aggregates by macroautophagy. Int J Cell Biol. 2012;2012:736905.
19. González-Rodríguez A, Mayoral R, Agra N, Valdecantos MP, Pardo V, Miquilena-Colina ME, Vargas-Castrillón J, Lo Iacono O, Corazzari M, Fimia GM, et al. Impaired autophagic flux is associated with increased endoplasmic reticulum stress during the development of NAFLD. Cell Death Dis. 2014;5:e1179.
20. Liu HY, Han J, Cao SY, Hong T, Zhuo D, Shi J, Liu Z, Cao W. Hepatic autophagy is suppressed in the presence of insulin resistance and hyperinsulinemia: inhibition of FoxO1-dependent expression of key autophagy genes by insulin. J Biol Chem. 2009;284:31484–92.
21. Yang L, Li P, Fu S, Calay ES, Hotamisligil GS. Defective hepatic autophagy in obesity promotes ER stress and causes insulin resistance. Cell Metab. 2010;11:467–78.
22. Meroni M, De Caro E, Chiappori F, Longo M, Paolini E, Mosca E, Merelli I, Lombardi R, Badiali S, Maggioni M, et al. Hepatic and adipose tissue transcriptome analysis highlights a commonly deregulated autophagic pathway in severe MASLD. Obes (Silver Spring). 2024;32:923–37.
23. Schlosser G, Patthey C, Shimeld SM. The evolutionary history of vertebrate cranial placodes II. Evolution of ectodermal patterning. Dev Biol. 2014;389:98–119.
24. Stampfli AR, Blankenfeldt W, Seebeck FP. Structural basis of ergothioneine biosynthesis. Curr Opin Struct Biol. 2020;65:1–8.
25. Heath H, Toennies G. The preparation and properties of ergothioneine disulphide. Biochem J. 1958;68:204–10.
26. Sao Emani C, Gallant JL, Wiid IJ, Baker B. The role of low molecular weight thiols in Mycobacterium tuberculosis. Tuberculosis (Edinb). 2019;116:44–55.
27. Borodina I, Kenny LC, McCarthy CM, Paramasivan K, Pretorius E, Roberts TJ, van der Hoek SA, Kell DB. The biology of ergothioneine, an antioxidant nutraceutical. Nutr Res Rev. 2020;33:190–217.
28. Cheah IK, Halliwell B. Ergothioneine; antioxidant potential, physiological function and role in disease. Biochim Biophys Acta. 2012;1822:784–93.
29. Cheah IK, Halliwell B. Ergothioneine, recent developments. Redox Biol. 2021;42:101868.
30. Cheah IK, Tang RM, Yew TS, Lim KH, Halliwell B. Administration of pure ergothioneine to healthy human subjects: Uptake, Metabolism, and effects on biomarkers of oxidative damage and inflammation. Antioxid Redox Signal. 2017;26:193–206.
31. Mayayo-Vallverdú C, López de Heredia M, Prat E, González L, Espino Guarch M, Vilches C, Muñoz L, Asensi MA, Serra C, Llebaria A, et al. The antioxidant l-Ergothioneine prevents cystine lithiasis in the Slc7a9(-/-) mouse model of cystinuria. Redox Biol. 2023;64:102801.
32. Tang RMY, Cheah IK, Yew TSK, Halliwell B. Distribution and accumulation of dietary ergothioneine and its metabolites in mouse tissues. Sci Rep. 2018;8:1601.
33. Ashraf NU, Sheikh TA. Endoplasmic reticulum stress and oxidative stress in the pathogenesis of non-alcoholic fatty liver disease. Free Radic Res. 2015;49:1405–18.
34. Cobbina E, Akhlaghi F. Non-alcoholic fatty liver disease (NAFLD) - pathogenesis, classification, and effect on drug metabolizing enzymes and transporters. Drug Metab Rev. 2017;49:197–211.
35. Fu TT, Shen L. Ergothioneine as a natural antioxidant against oxidative stress-related diseases. Front Pharmacol. 2022;13:850813.
36. Turck D, Bresson JL, Burlingame B, Dean T, Fairweather-Tait S, Heinonen M, Hirsch-Ernst KI, Mangelsdorf I, McArdle HJ, Naska A, et al. Statement on the safety of synthetic l-ergothioneine as a novel food - supplementary dietary exposure and safety assessment for infants and young children, pregnant and breastfeeding women. Efsa j. 2017;15:e05060.
37. Poitout V, Robertson RP. Glucolipotoxicity: fuel excess and beta-cell dysfunction. Endocr Rev. 2008;29:351–66.
38. Lee HJ, Yang SJ. Nicotinamide riboside regulates inflammation and mitochondrial markers in AML12 hepatocytes. Nutr Res Pract. 2019;13:3–10.
39. Zhang CY, Tan XH, Yang HH, Jin L, Hong JR, Zhou Y, Huang XT. COX-2/sEH dual inhibitor alleviates hepatocyte senescence in NAFLD mice by restoring autophagy through Sirt1/PI3K/AKT/mTOR. Int J Mol Sci. 2022;23:8267.
40. Sorice M. Crosstalk of Autophagy and apoptosis. Cells. 2022;11:1479.
41. Chaudhari N, Talwar P, Parimisetty A, Lefebvre d'Hellencourt C, Ravanan P. A molecular web: endoplasmic reticulum stress, inflammation, and oxidative stress. Front Cell Neurosci. 2014;8:213.
42. Deretic V. Autophagy in inflammation, infection, and immunometabolism. Immunity. 2021;54:437–53.
43. Gao Q. Oxidative stress and Autophagy. Adv Exp Med Biol. 2019;1206:179–98.
44. Prerna K, Dubey VK. Beclin1-mediated interplay between autophagy and apoptosis: New understanding. Int J Biol Macromol. 2022;204:258–73.
45. Tran S, Fairlie WD, Lee EF. BECLIN1: protein structure, function and regulation. Cells. 2021;10:1522.
46. Wang F, Peters R, Jia J, Mudd M, Salemi M, Allers L, Javed R, Duque TLA, Paddar MA, Trosdal ES, et al. ATG5 provides host protection acting as a switch in the atg8ylation cascade between autophagy and secretion. Dev Cell. 2023;58:866–e884868.

47. Changotra H, Kaur S, Yadav SS, Gupta GL, Parkash J, Duseja A. ATG5: a central autophagy regulator implicated in various human diseases. Cell Biochem Funct. 2022;40:650–67.
48. Sadeghi A, Shabani M, Alizadeh S, Meshkani R. Interplay between oxidative stress and autophagy function and its role in inflammatory cytokine expression induced by palmitate in skeletal muscle cells. Cytokine. 2020;125:154835.

Publisher's note